Combustion, Explosion, and Shock Waves, Vol. 46, No. 5, pp. 491–506, 2010

Syngas Oxidation Mechanism

A. M. Starik,[1] N. S. Titova,[1] A. S. Sharipov,[1] and V. E. Kozlov[1]

UDC 544.452:544:324,544.431.7

Translated from *Fizika Goreniya i Vzryva*, Vol. 46, No. 5, pp. 3–19, September–October, 2010.
Original article submitted October 14, 2009.

A comprehensive analysis of synthesis gas (syngas) oxidation kinetics in wide ranges of temperature, pressure, fuel-to-air equivalence ratio, and fuel composition is performed on the basis of the reaction mechanism of syngas ignition and combustion in air. A vast set of experimental data on the ignition delay time, laminar flame propagation velocity, and time evolution of mole fractions of the basic species, which were obtained in shock tubes and in a flow reactor, is used for verification of the kinetic model. Based on a sensitivity analysis, it is shown that the role of reactions determining the basic characteristics of ignition and combustion depends on the composition of the fuel–air mixture and the syngas proper.

Key words: syngas, hydrogen, chemical kinetics, ignition, combustion.

INTRODUCTION

The possibility of using alternative fuels both in power engineering and in engines of various transportation systems has been intensely discussed recently. Particular attention of researchers is focused on the so-called synthetic fuels formed during coal gasification or partial gasification of saturated and non-saturated hydrocarbons whose composition mainly includes molecular hydrogen and carbon oxide [1]. Depending on the method of production of such a synthetic fuel (it is usually called the synthesis gas or syngas), the ratio of these two species can vary within wide limits. Though the kinetics of oxidation of each species in the syngas (H_2 and CO) is rather well known and detailed kinetic models have been developed to describe ignition and combustion of H_2–O_2 (air) and CO–O_2 (air) mixtures [2–8], many problems inherent in the correct description of syngas oxidation kinetics have not been solved yet [9, 10]. [In what follows, the expression of the type "H_2–O_2 (air)" means that either O_2 or air is used; the same refers to "... + N_2 (He)".]

It should be noted that the reaction mechanism of oxidation of the H_2–CO mixture is the basic mechanism for constructing kinetic models of ignition and combustion of almost all hydrocarbons, i.e., an adequate description of the processes in the H_2–CO–O_2 (air) mixture is extremely important for understanding the kinetics of chain reactions in more complicated fuel–air systems [9]. That is why significant recent efforts have been applied to experimental investigations of syngas ignition and combustion processes [11–15] and to creation of extended reaction mechanisms [16–18] that ensure an adequate description of these experiments. These models have been developed owing to significant progress in more accurate calculations and measurements of the rate constants of elementary reactions, in determining the thermodynamic properties of individual substances, and also in measuring the characteristics of combustion processes, such as the ignition delay time and the flame propagation velocity in the H_2–CO–O_2 (air) mixture. Nevertheless, despite significant achievements in the development of the kinetic mechanism of ignition and combustion of H_2–O_2 and CO–O_2 mixtures, the list of reactions in the oxidation mechanism of both hydrogen and carbon oxide is far from being complete. For instance, the above-mentioned kinetic models do not include reactions with participation of O_3, which are necessary to describe the processes of oxidation and ignition of various mixtures containing hydrogen, hydrocarbons, and ozone.

[1]Baranov Central Institute of Aviation Motors, Moscow 111116; star@ciam.ru.

TABLE 1

List of Reactions Included into the Model and Rate Constants of these Reactions

No.	Reaction	k_+, $(\mathrm{cm}^3/\mathrm{mole})^{n-1}\cdot\mathrm{sec}^{-1}$			k_-, $(\mathrm{cm}^3/\mathrm{mole})^{n-1}\cdot\mathrm{sec}^{-1}$			Reference
		A	n	E_a, K	A	n	E_a, K	
Reactions with O_2, H_2, O, H, OH, and H_2O								
1	$H_2O + H = OH + H_2$	$8.4\cdot10^{13}$	0	10,116	$2\cdot10^{13}$	0	2600	[6]
2	$O_2 + H = OH + O$	$2.2\cdot10^{14}$	0	8455	$1.3\cdot10^{13}$	0	350	[21]
3	$H_2 + O = OH + H$	$1.8\cdot10^{10}$	1	4480	$8.3\cdot10^{9}$	1	3500	[6]
4	$O_2 + M = 2O + M$	$5.4\cdot10^{18}$	−1	59,400	$6\cdot10^{13}$	0	−900	[6]
5	$H_2 + M = 2H + M$	$2.2\cdot10^{14}$	0	48,300	$9\cdot10^{17}$	−1	0	[6]
6	$H_2O + M = OH + H + M$	$1\cdot10^{24}$	−2.2	59,000	$2.2\cdot10^{22}$	−2	0	[6]
7	$OH + M = O + H + M$	$8.5\cdot10^{18}$	−1	50,830	$7.1\cdot10^{18}$	−1	0	[6]
8	$H_2O + O = 2OH$	$5.8\cdot10^{13}$	0	9059	$5.3\cdot10^{12}$	0	503	[6]
Reactions with HO_2								
9	$H + O_2(+M) = HO_2(+M)$	$3.5\cdot10^{16}$	−0.41	−565	—	—	—	[2]
	$F_c(N_2) = 0.5$	$1.48\cdot10^{12}$	0.6	0				
10	$H_2 + O_2 = H + HO_2$	$7.39\cdot10^{5}$	2.43	26,926	—	—	—	[20]
11	$H_2O + O = H + HO_2$	$4.76\cdot10^{11}$	0.372	28,743	$1\cdot10^{13}$	0	540	[6]
12	$H_2O + O_2 = OH + HO_2$	$1.5\cdot10^{15}$	0.5	36,600	$3\cdot10^{14}$	0	0	[6]
13	$2OH = H + HO_2$	$1.2\cdot10^{13}$	0	20,200	$2.5\cdot10^{14}$	0	950	[6]
14	$OH + O_2 = O + HO_2$	$1.3\cdot10^{13}$	0	28,200	$5\cdot10^{13}$	0	500	[6]
Reactions with H_2O_2								
15	$H + H_2O_2 = H_2 + HO_2$	$1.7\cdot10^{12}$	0	1900	$6\cdot10^{11}$	0	9300	[6]
16	$H + H_2O_2 = H_2O + OH$	$5\cdot10^{14}$	0	5000	$2.4\cdot10^{14}$	0	40,500	[6]
17	$2HO_2 = H_2O_2 + O_2$	$1.8\cdot10^{13}$	0	500	$3\cdot10^{13}$	0	21,600	[6]
18	$HO_2 + H_2O = H_2O_2 + OH$	$1.8\cdot10^{13}$	0	15,100	$1\cdot10^{13}$	0	910	[6]
19	$OH + HO_2 = H_2O_2 + O$	$5.2\cdot10^{10}$	0.5	10,600	$2\cdot10^{13}$	0	2950	[6]
20	$H_2O_2 + M = 2OH + M$	$1.2\cdot10^{17}$	0	22,900	$9.1\cdot10^{14}$	0	−2650	[6]
Reactions with O_3								
21	$O_3 + M = O_2 + O + M$	$4\cdot10^{14}$	0	11,400	$6.9\cdot10^{12}$	0	−1050	[6]
22	$O_3 + H = OH + O_2$	$2.3\cdot10^{11}$	0.75	0	$4.4\cdot10^{7}$	1.44	38,600	[6]
23	$O_3 + O = 2O_2$	$1.1\cdot10^{13}$	0	2300	$1.2\cdot10^{13}$	0	50,500	[6]
24	$O_3 + OH = HO_2 + O_2$	$9.6\cdot10^{11}$	0	1000	—	—	—	[6]
25	$O_3 + H_2 = OH + HO_2$	$6.02\cdot10^{10}$	0	10,000	—	—	—	[6]
26	$O_3 + HO_2 = OH + 2O_2$	$2\cdot10^{10}$	0	1000	—	—	—	[6]
Reactions with CO								
27	$CO + O_2 = CO_2 + O$	$3.2\cdot10^{11}$	0	18,950	$2.8\cdot10^{12}$	0	22,090	[19]
28	$CO + O\ (+M) = CO_2\ (+M)$	$1.55\cdot10^{24}$ $1.8\cdot10^{10}$	−2.79 0	2118 1205	—	—	—	[17]
29	$CO + OH = H + CO_2$	$1.51\cdot10^{7}$	1.3	−388.1	$1.7\cdot10^{9}$	1.3	10,876.3	[6]
30	$CO + HO_2 = OH + CO_2$	$1.15\cdot10^{5}$	2.28	8849	—	—	—	[16]

TABLE 1 (Final)

No.	Reaction	k_+, $(\text{cm}^3/\text{mole})^{n-1} \cdot \text{sec}^{-1}$			k_-, $(\text{cm}^3/\text{mole})^{n-1} \cdot \text{sec}^{-1}$			Reference
		A	n	E_a, K	A	n	E_a, K	
	Reactions with HCO							
31	HCO + M = H + CO + M H_2/2.5/H_2O/6/CO/1.9/CO_2/3.8	$4.75 \cdot 10^{11}$	0.7	7513	—	—	—	[18]
32	HCO + H_2 = CH_2O + H	$2.63 \cdot 10^{13}$	0	12,686	$5.01 \cdot 10^{13}$	0	2016	[19]
33	CO + HO_2 = HCO + O_2	$8.91 \cdot 10^{12}$	0	16,274	$3.02 \cdot 10^{12}$	0	0	[19]
34	CO + H_2 = HCO + H	$1.32 \cdot 10^{15}$	0	45,360	$1.2 \cdot 10^{14}$	0	0	[19]
35	HCO + O = H + CO_2	$3.01 \cdot 10^{13}$	0	0	—	—	—	[19]
36	HCO + O = OH + CO	$1 \cdot 10^{14}$	0	0	$2.88 \cdot 10^{14}$	0	44,302	[19]
37	HCO + OH = H_2O + CO	$3.16 \cdot 10^{13}$	0	0	$8.91 \cdot 10^{14}$	0	52,970	[19]
38	2HCO = H_2 + 2CO	$3.01 \cdot 10^{12}$	0	0	—	—	—	[19]
	Reactions with CH_2O							
39	2HCO = CH_2O + CO	$1.81 \cdot 10^{13}$	0	0	—	—	—	[19]
40	CH_2O + M = H + HCO + M	$3.31 \cdot 10^{16}$	0	40,824	$1.41 \cdot 10^{11}$	1	−5947	[19]
41	CH_2O + O_2 = HO_2 + HCO	$3.63 \cdot 10^{15}$	0	23,204	$1 \cdot 10^{14}$	0	1512	[19]
42	CH_2O + O = HCO + OH	$5.01 \cdot 10^{13}$	0	2318	$1.74 \cdot 10^{12}$	0	8654	[19]
43	CH_2O + OH = HCO + H_2O	$3.47 \cdot 10^{9}$	1.2	−242	$1.17 \cdot 10^{9}$	1.2	14,802	[19]
44	CH_2O + HO_2 = H_2O_2 + HCO	$2 \cdot 10^{11}$	0	4032	$2.19 \cdot 10^{10}$	0	3321	[19]

Note. For reaction No. 9, upper value k_0 and lower value k_∞; for reaction No. 28, upper value k_0 and lower value k_{inf}.

The objective of this paper is to develop a kinetic model of processes in the H_2–CO–O_2 (air) mixture, which would provide a reasonably accurate description of available experimental data on the ignition delay time and laminar flame velocity.

1. KINETIC MODEL

The reaction mechanism developed in this work includes 44 reversible reactions with the following components: H_x (x = 1, 2), O_y (y = 1, 2, 3), HO_x, H_2O, H_2O_2, CO_x, HCO, and CH_2O. This mechanism is based on the previously developed models of ignition of the H_2–O_2 (air) [6] and CH_4–O_2 (air) [19] mixtures. Table 1 gives the list of reactions included into the model and the coefficients of the Arrhenius dependence of the rate constant of the qth reaction $k_q = A_q T^{n_q} \exp(-E_{a,q}/T)$, where A_q is the pre-exponential factor, $E_{a,q}$ is the activation energy of the qth reaction, n_q is the power index, and T is the temperature; these data were chosen on the basis of recommendations given in [2, 6, 16–23]. The backward reactions, for which the rate constants are not given in Table 1, are calculated based on the principle of detailed balance. The necessary thermodynamic data were borrowed from [24, 25].

As the syngas oxidation process follows the chain mechanism, particular attention in choosing the reaction rate constants is paid to reactions of chain initiation, propagation, and termination. The main reaction of chain initiation in H_2–O_2 (air) and H_2–CO–O_2 (air) mixtures is the reaction $H_2 + O_2 = H + HO_2$ (reaction No. 10; hereinafter, the reaction numbers used in the text coincide with those in Table 1). The expression for the rate constant of this reaction was proposed in [20], based on the analysis of experimental data and *ab initio* calculations. It is exactly this expression for $k_{+10}(T)$ that is used in most currently known reaction mechanisms of ignition and combustion of the H_2–O_2 (air) mixtures.

An important reaction, which determines the development of the chain mechanism to a large extent, is the chain branching reaction $O_2 + H = OH + O$ (reaction No. 2). In our model, as well as in [3], its kinetic parameters were determined in accordance with the modern data [21]. Figure 1 shows the temperature dependences of the rate constants of this process, which are used in various reaction mechanisms. The dependences $k_{+2}(T)$ are seen to be very close to each other. It should be noted, however, that the ignition delay time (induction period) τ_{in} is extremely sensitive to the value of k_{+2}, and even a minor change in the

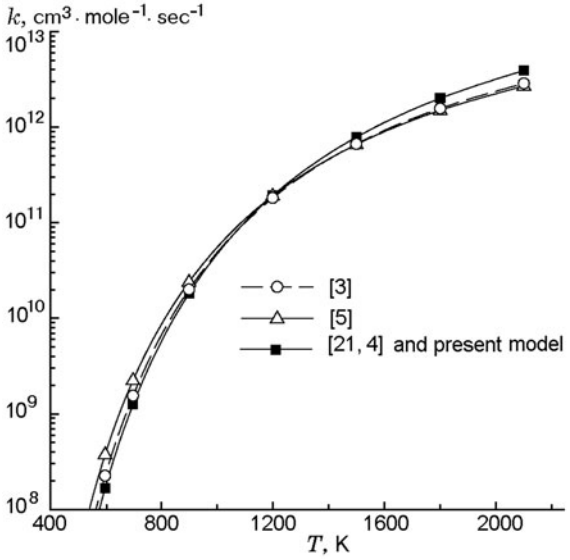

Fig. 1. Rate constants of the reaction $H_2 + O = OH + H$ used in different kinetic models versus temperature.

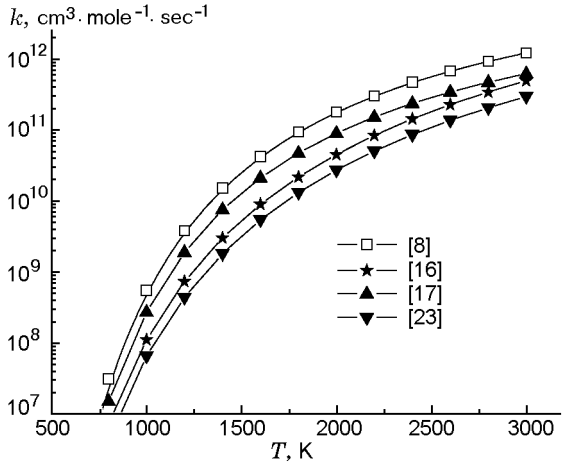

Fig. 2. Rate constants of the reaction $CO + HO_2 = OH + CO_2$ used in different kinetic models and calculated by the theory of an activated complex with the use of *ab initio* calculations in [16] and [23] versus temperature.

latter leads to a large change in τ_{in} in both H_2–O_2 (air) and H_2–CO–O_2 (air) mixtures.

The rate constant of the second significant reaction of chain branching (reaction No. 3) $O + H_2 = OH + H$ was also found quite accurately in a wide range of temperatures [22]. An approximation for $k_{+3}(T)$ very close to approximations [2] and [5] is used in our work.

The next extremely important reaction in hydrogen–oxygen mixtures is the chain termination reaction $H + O_2 + M = HO_2 + M$ (reaction No. 9). It is this process that is responsible for elimination of H atoms, which are carriers of the chain mechanism in reactive mixtures. Particular attention to choosing the rate constant of this reaction was paid in [2]. Therefore, the rate constant of reaction No. 9 recommended in [2] is used in our reaction mechanism.

If CO molecules are added to the hydrogen–air mixture, there appear new important channels governing the evolution of the chain mechanism. These are the chain propagation reactions $CO + OH = H + CO_2$ and $CO + HO_2 = OH + CO_2$ (reaction Nos. 29 and 30) and the chain termination reactions $CO + O + M = CO_2 + M$ and $H + CO + M = HCO + M$ (reaction Nos. 28 and 31). Particular attention in creating kinetic models of syngas oxidation is paid to choosing the rate constants of these reactions [9]. The experiments [11] showed, for instance, that the ignition delay time τ_{in} in the H_2–CO–O_2 mixture substantially depends on the ratio of H_2 and CO mole fractions, though the calculations performed even by relatively advanced models [7, 17] do not predict such a dependence. Mittal et al. [11] put forward a hypothesis that the rate constant of reaction No. 30 is unduly overestimated in modern models and that is why the models [7, 17] cannot explain the dependence of τ_{in} on the ratio of H_2 and CO mole fractions in the syngas. Sun et al. [16] determined the rate constant of this reaction from the theory of the activated complex with allowance for *ab initio* calculations of geometry and parameters of the transitional state $CO + HO_2$. This rate constant is used in the present model. Figure 2 shows the dependences $k_{+30}(T)$ recommended in various publications. It is seen that, for instance, at $T = 1000$ K, there is a tenfold scatter in the values of k_{+30}. The calculations show that the rate constant of this reaction recommended in [16] ensures the best agreement with experimental data, especially on the flame propagation velocity in H_2–CO–air mixtures with different fractions of CO and H_2. The sensitivity analysis also shows that reaction No. 31 is very important for the description of the flame propagation velocity. The rate constant for this reaction is determined in accordance with the recommendations given by Li et al. [18].

2. COMPARISON WITH EXPERIMENTAL DATA

Naturally, any kinetic model has to describe available experimental data on the ignition delay time, flame propagation velocity, and evolution of various species in time. As the syngas contains H_2 and CO whose

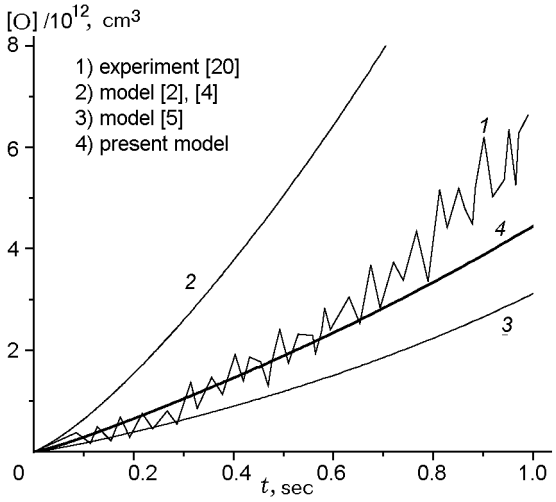

Fig. 3. Time evolution of the mole fraction of O atoms measured in [20] and calculated by different models for the H_2–O_2–Kr mixture behind the reflected shock wave at $T_0 = 1981$ K, $p_0 = 64.7$ kPa, and initial mole fractions $\gamma_{H_2} = 2.68 \cdot 10^{-5}$ and $\gamma_{O_2} = 0.0659$.

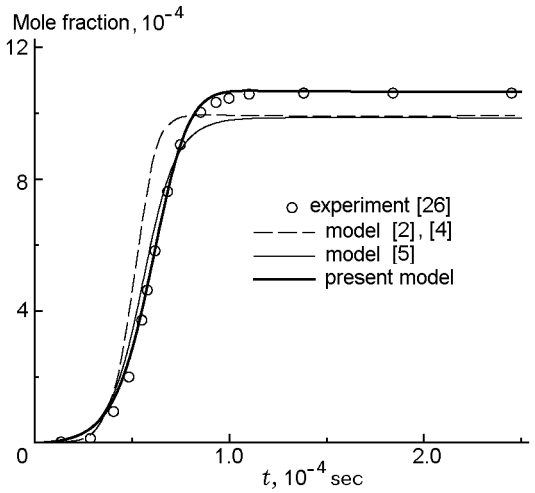

Fig. 4. Time evolution of the mole fraction of OH radicals measured in [26] and calculated by different models for the H_2–O_2–Ar mixture behind the reflected shock wave at $T_0 = 2590$ K, $p_0 = 1$ atm, $\gamma_{H_2} = 4.0 \cdot 10^{-3}$, and $\gamma_{O_2} = 4.0 \cdot 10^{-3}$.

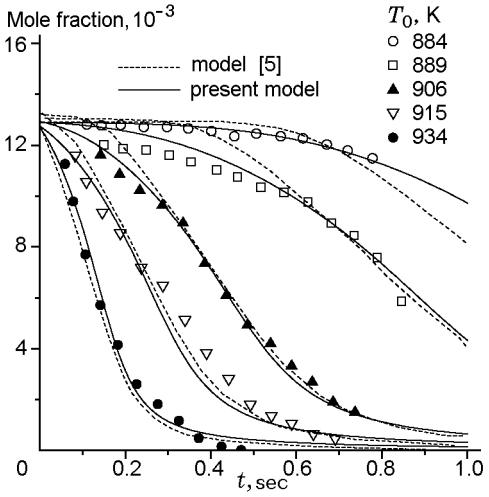

Fig. 5. Time evolution of the mole fraction of H_2 measured in [2] and calculated by the mechanism [5] and by the present model for the 1.33% H_2–2.21% O_2–N_2 mixture ($p_0 = 6.5$ atm) with different values of the initial temperature.

mole fractions can vary in rather wide ranges, obviously, the kinetic models developed to describe syngas ignition and combustion should accurately describe experimental data for hydrogen–oxygen (air) mixtures as well.

2.1. Mole Fractions for Various Species

As the processes of ignition and combustion of H_2–CO–O_2 (air) mixtures follow the chain mechanism whose carriers are active O and H atoms and OH radicals, the reaction mechanism has to ensure a correct description of the time evolution of these species. The profile of the mole fraction of O atoms versus time, which was measured in [20] behind the shock wave reflected from the end face of the shock tube in an extremely lean hydrogen–oxygen mixture under conditions where no ignition occurs and the chain initiation process prevails is compared in Fig. 3 with the results calculated by the kinetic mechanisms [2], [4], and [5] and by the present model. (At time intervals smaller than the induction time τ_{in}, a good approximation in modeling the processes behind the reflected shock wave is known to be the constant volume approximation, which was also used in the present work.) It is seen that only our kinetic mechanism describes the experiment with sufficient accuracy. The mechanisms [2] and [4] substantially overestimate the mole fraction of O atoms measured in [20], while the model [5] predicts a slower increase in the mole fraction of atomic oxygen with time than that actually observed in the experiment.

The mole fraction of OH radicals behind the reflected shock wave in the course of ignition of the H_2–O_2–Ar mixture was measured in [26]. Figure 4 shows the time evolution of the OH mole fraction [26] and the dependences calculated with the use of different reaction mechanisms. It is seen that only the kinetic mechanism described in the present paper provides quantitative agreement with the experimental data.

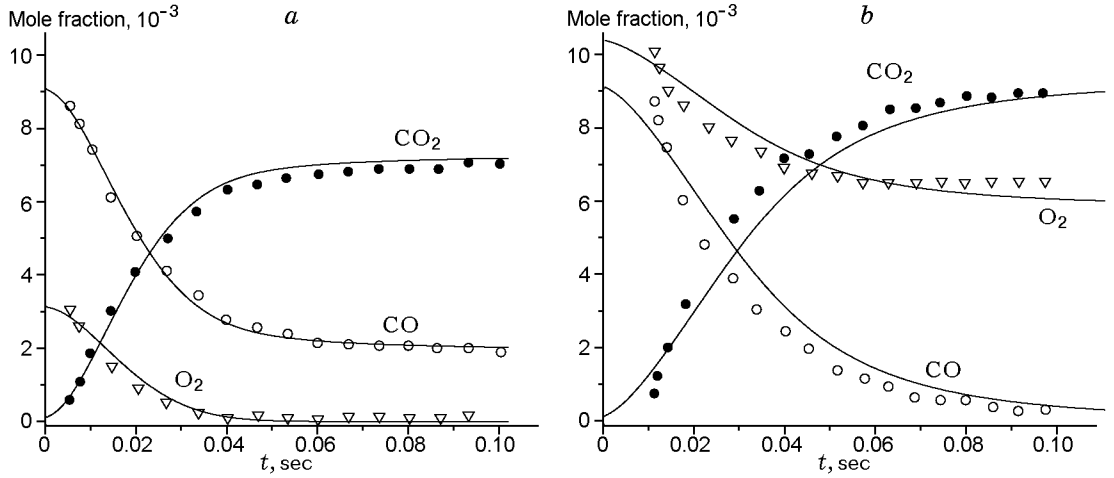

Fig. 6. Time evolution of the mole fractions of CO_2, CO, and O_2 for the 0.92% CO–0.59% H_2O–0.32% O_2 mixture in N_2 (T_0 = 1034 K and p_0 = 1 atm) (a) and 0.93% CO–0.58% H_2O–1.05% O_2 mixture in N_2 (T_0 = 1033 K and p_0 = 1 atm) (b) measured in [27] and calculated by the present model.

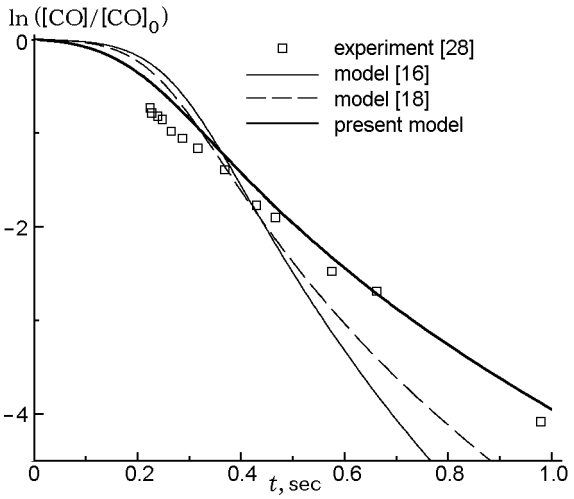

Fig. 7. Dimensionless concentration of CO molecules versus time during ignition of the 3.11 ppm CO–1.0% O_2–0.41% H_2O mixture in Ar (T_0 = 1273 K and p_0 = 1.22 atm).

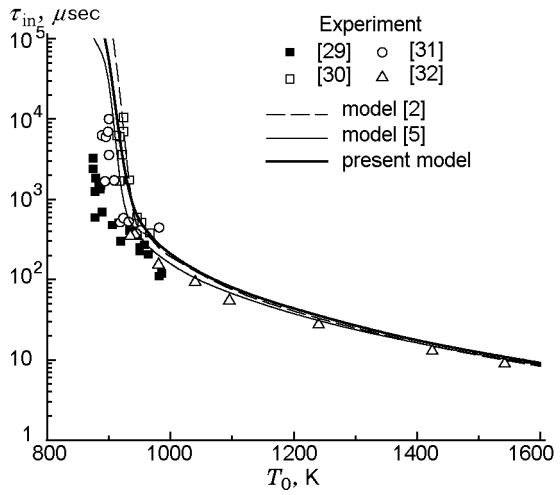

Fig. 8. Ignition delay time versus the initial temperature of the stoichiometric H_2–air mixture at p_0 = 1 atm.

Other measurements of the mole fractions of various species in H_2–O_2 (air) and CO–H_2O–O_2–Ar reactive mixtures were performed by the flow reactor technique [2, 27]. Figure 5 shows the time evolution of the mole fraction of H_2 in the 1.33% H_2–2.21% O_2–96.46% N_2 mixture with the initial pressure p_0 = 6.5 atm and different values of the temperature T_0, which were measured in [2] and calculated by the model [5]. The profiles of the mole fractions of CO_2, CO, and O_2 measured in [27] for the CO–H_2O–O_2–N_2 mixture with different mole fractions of O_2 and calculated by the present model are shown in Fig. 6. It is seen that the kinetic model developed in the present work provides an adequate description of the experimental data.

It should be noted that other modern kinetic models of syngas oxidation [16, 18] also allow the experiments [2, 27] to be described. For lean CO–H_2O–O_2–Ar mixtures, however, the results predicted by these models do not agree quantitatively with the experiment. Figure 7 shows the time evolution of the dimensionless concentration of CO in the case of oxidation of the CO–H_2O–O_2–Ar mixture in the flow reactor, which was measured in [28] and calculated with the use of different kinetic models. It is seen that the model developed in the present work offers a more accurate description of

the experimental data [28] than the models [16] and [18], which were specially adapted to describe the process of oxidation and combustion of the syngas in air.

2.2. Ignition Delay Time

Though the ignition delay measurements provide only information on the integral characteristic of the ignition process, i.e., the induction period τ_{in}, which is determined by the rate of formation of active radicals — carriers of the chain mechanism, nevertheless, the quantity τ_{in} is rather sensitive to the rate constants of the reactions involved into this process [2, 5, 9] and gives a certain idea about the rate of chain process development. The measurements of τ_{in} are mainly performed in shock tubes behind the shock wave reflected from the end face of the tube. Such experiments for H_2–O_2(air)–Ar and H_2–CO–O_2(air)–Ar mixtures have been performed in wide ranges of temperatures ($T_0 = 870$–2700 K) and pressures ($p_0 = 0.5$–66 atm) for lean ($\phi < 1$), stoichiometric ($\phi = 1$), and rich ($\phi > 1$) compositions. Figure 8 shows the data [29–32] measured in a stoichiometric mixture of H_2 with air at atmospheric pressure and the results calculated by the reaction mechanisms [2], [5], and the present model. It is seen that the predictions of all kinetic mechanisms fit the experimental data well and are close to each other. As the ignition under the conditions considered ($p_0 = 1$ atm and $T_0 = 920$–1600 K) is mainly determined by the chain branching rate, we can conclude that all reaction mechanisms considered in the paper provide a satisfactory description of the chain branching process.

At pressures above the atmospheric value ($p_0 = 2$ atm), however, there appear certain differences between the predictions of different models. As is seen from Fig. 9, the mechanisms [4], [5], and the present model provide good agreement with the experiments [33, 34] for the stoichiometric H_2–air mixture, whereas the model [2] is inconsistent with the experiment at $T < 1050$ K.

The same situation is observed during syngas ignition. At $p_0 > 1.5$ atm, there are significant differences in ignition delay times calculated by different models. These differences are illustrated in Fig. 10, which shows the times needed for the mole fraction of CO_2 to reach the values of $2.1 \cdot 10^{-3}$ and $5.66 \cdot 10^{-3}$ during ignition of the H_2–CO–O_2–Ar mixture with $p_0 = 1.4$–2.2 atm and different values of T_0. It is seen that the reaction mechanisms [16] and [18] systematically underestimate the values of the times registered in the experiment [35]. The difference between the experiment and calculation

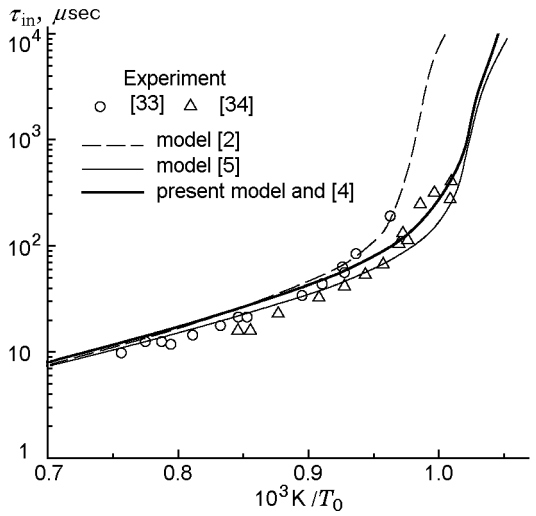

Fig. 9. Ignition delay time versus temperature for the stoichiometric H_2–air mixture at $p_0 = 2$ atm.

increases with decreasing initial temperature of the mixture and reaches 30–35% at $T_0 = 2050$ K. Our model ensures a more accurate description of the experimental data, and the difference between the calculation and experiment stays within 12% even at $T_0 = 2050$ K. At pressures below the atmospheric value, the difference in the values of τ_{in} in the H_2–CO–O_2 (air) mixture calculated by the kinetic models [16] and [18] and by the model developed in the present work becomes insignificant. This fact is illustrated in Fig. 11, which shows the results calculated by these models and the value of $[O_2] \cdot \tau_{\text{in}}$ measured in the experiments [36], where $[O_2]$ is the concentration of O_2 molecules in the H_2–CO–O_2–Ar mixture ($p_0 = 0.225$ atm).

The situations described above refer to stoichiometric mixtures. It is also important to describe experimental data on the ignition delay time for lean and rich mixtures. The values of τ_{in} measured in a lean mixture in the temperature range $920 \leqslant T_0 \leqslant 1050$ K were reported in [30]. Figure 12 shows the dependence $\tau_{\text{in}}(T_0)$ for the H_2–air mixture with $\phi = 0.5$ and 0.75 at $p = 1$ atm. It is seen that the experimental results on the ignition delay time are very well predicted by the reaction mechanism [5] and the present model for $\phi = 0.5$, whereas the kinetic mechanism [2] overpredicts the values of τ_{in}. The best agreement with the experiment for the mixture with $\phi = 0.75$ is ensured by the present model. The reaction mechanism [5] underpredicts the ignition delay time at $T_0 < 950$ K, while the mechanism [2], vice versa, predicts substantially higher values of τ_{in} at $T_0 \leqslant 1000$ K than those measured in the experiment. There are some available experimental data on the ignition delay time for H_2–O_2–Ar and

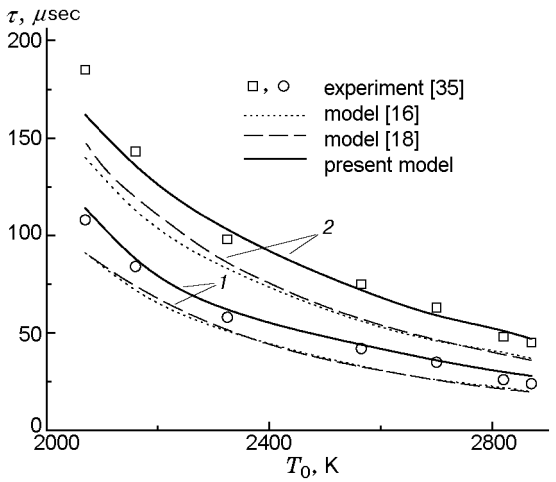

Fig. 10. Times necessary to reach the mole fractions $\gamma_{CO_2} = 2.1 \cdot 10^{-3}$ (1) and $5.66 \cdot 10^{-3}$ (2) for the 0.05% H_2–12.17% CO–1% O_2–86.78% Ar mixture ($p_0 = 1.4$–2.2 atm) at different initial temperatures, which were obtained in the experiment and calculated by different models.

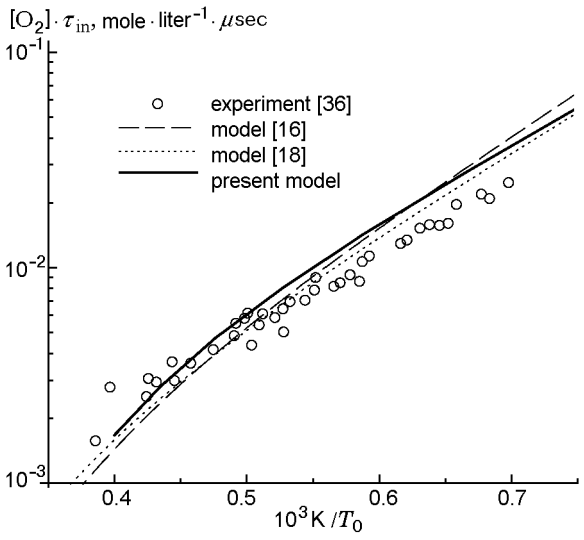

Fig. 11. Dependences of $[O_2] \cdot \tau_{in}$ on temperature for the 1% H_2–3% CO–5% O_2–91% Ar mixture ($p = 2.25 \cdot 10^4$ Pa), which were obtained in the experiment and calculated by different models: τ_{in} is the time instant when the OH mole fraction reaches $2.5 \cdot 10^{-10}$ mole/cm^3.

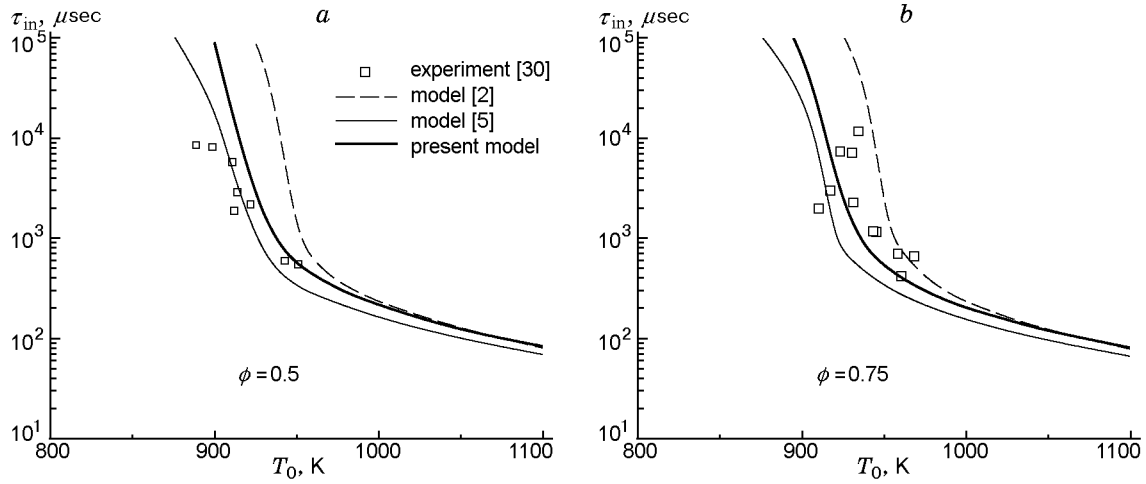

Fig. 12. Ignition delay times for the H_2–air mixture versus temperature at $p_0 = 1$ atm.

CO–H_2–O_2–Ar mixtures, including experiments at high pressures ($p_0 = 33$ and 57 atm). Figure 13 shows the times τ_{in} as functions of T_0 for a stoichiometric H_2–O_2–Ar mixture, which were measured in [37] and calculated by different reaction mechanisms. All reaction mechanisms analyzed in this work yield extremely close values of τ_{in} at these parameters are ensure an adequate description of the experiment.

In contrast to the hydrogen–oxygen mixture, an increase in pressure in the H_2–CO–O_2–Ar mixture enhances the difference between the calculated and experimental values of τ_{in}. This is clearly seen in Fig. 14, which shows the values of τ_{in} as a function of the CO fraction in the fuel, which were obtained in the experiment [11] at $p_0 = 15$ and 50 atm and calculated by our model and by the model [17]. Though our model describes the experimental data much better than the

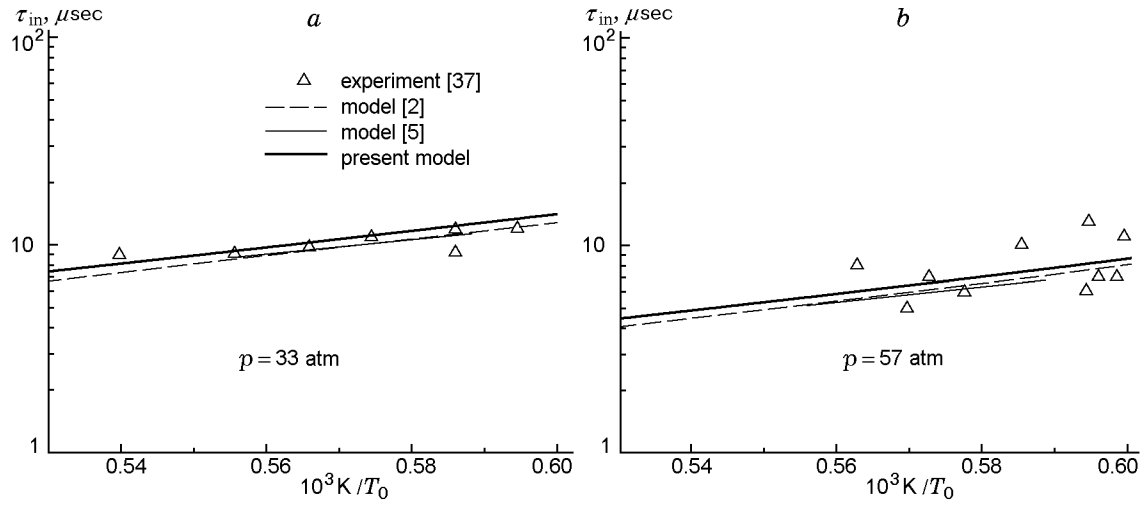

Fig. 13. Ignition delay times for the 0.5% H_2–0.25% O_2–99.25% Ar mixture.

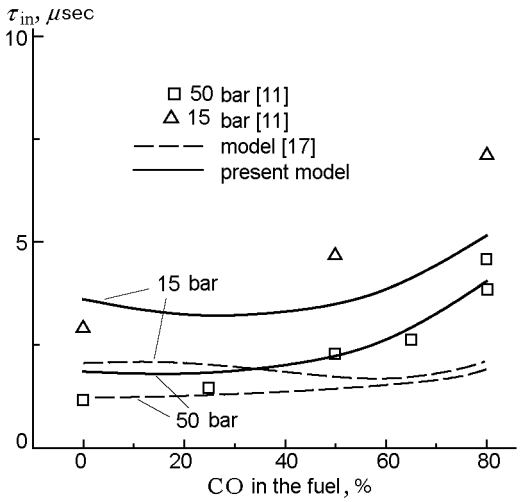

Fig. 14. Ignition delay times for the 12.6% (CO + H_2)–6.3% O_2–18.2% N_2–62.9% Ar mixture versus the fraction of CO in the fuel at $p_0 = 15$ bar ($T_0 = 1035.5$ K) and $p_0 = 50$ bar ($T_0 = 1040$ K).

model [17], it still underpredicts (by 30%) the values of τ_{in} at high CO fractions in the syngas and $p_0 = 15$ atm.

It is of interest to find which reactions, depending on the CO fraction in the syngas, prevail in the induction period and dominate in the course of ignition of the H_2–CO–O_2 (air) mixture. Figure 15 shows the time evolution of the reaction rates for the test conditions [11] ($p_0 = 50$ atm and $T_0 = 1040$ K). The concentrations of the species and the gas temperature for the mixture containing 20 and 80% of CO in the syngas are shown in Fig. 16. It is seen from these distributions that the process of formation of active O and H atoms and OH radicals proceeds in a different manner, depending on the CO concentration, though the reactions governing this process and, hence, ignition of the mixture are certainly identical, regardless of the CO fraction (20 or 80%). The basic reaction of chain initiation in both cases is the reaction of carbon monoxide oxidation CO + O_2 = CO_2 + O (reaction No. 27) in which atomic oxygen is formed. Further, it participates in the chain branching reaction H_2 + O = OH + H (reaction No. 3) in which the H atom is formed in addition to the OH radical. Atomic hydrogen, in turn, enters the recombination reaction H + O_2 + M = HO_2 + M (reaction No. 9), which leads to chain termination. At moderate gas temperatures ($T_0 \approx 1000$ K), reaction No. 9 proceeds faster than reaction No. 3, and no ignition occurs at this stage. It is of interest to note that the rate of reaction No. 27 in the case of an increased fraction of CO in the syngas (80%) is higher than in the case of a

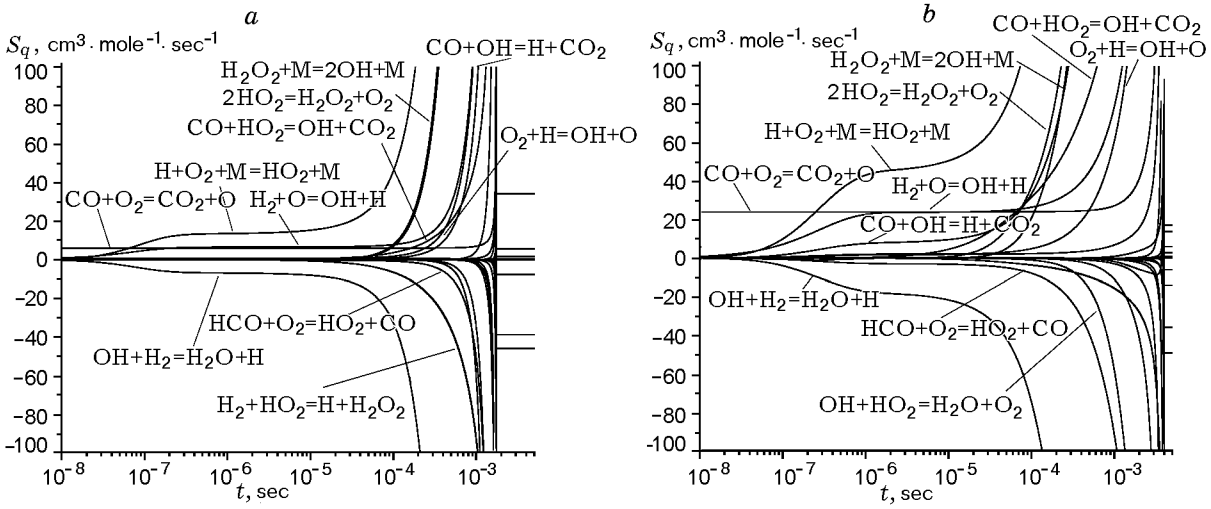

Fig. 15. Reaction rates in the 12.6% (CO + H_2)–6.3% O_2–18.2% N_2–62.9% Ar mixture at $p_0 = 50$ atm, $T_0 = 1040$ K, and CO fraction in the syngas equal to 20 (a) and 80% (b).

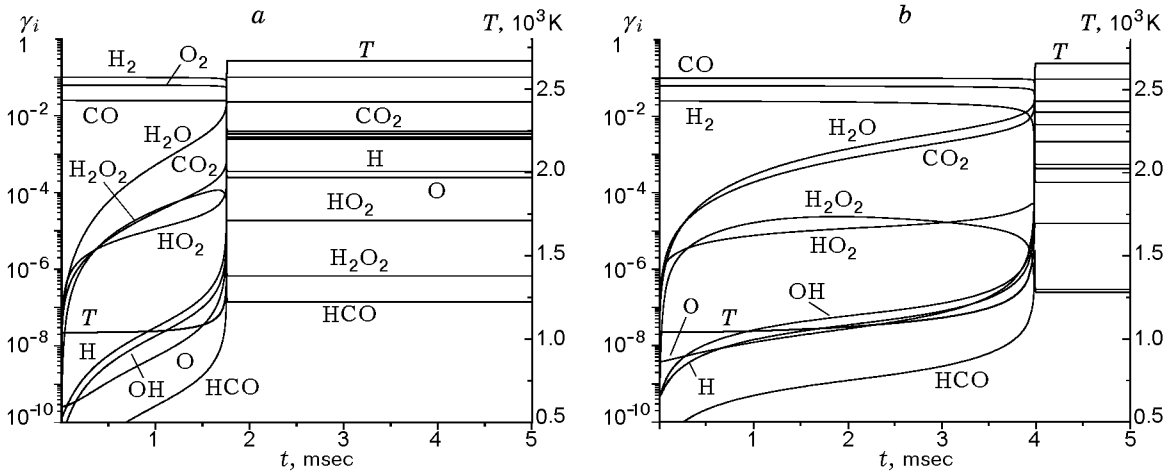

Fig. 16. Concentrations of the species and gas temperatures for the 12.6% (CO + H_2)–6.3% O_2–18.2% N_2–62.9% Ar mixture at $p_0 = 50$ atm, $T_0 = 1040$ K, and CO fraction in the syngas equal to 20 (a) and 80% (b).

reduced CO concentration (20%), and the mole fraction of atomic oxygen at the initial stage is also higher in the case of a higher CO concentration. The rate of the chain termination reaction No. 9, however, is also higher in this case. When H atoms, OH radicals, and HO_2 are formed, they participate in the reactions OH + H_2 = H_2O + H, $2HO_2 = H_2O_2 + O_2$, $H_2O_2 + M = 2OH + M$, CO + OH = H + CO_2, and HCO + O_2 = HO_2 + CO. Yet, production of active O and H atoms and OH radicals in these processes is rather slow, and their concentrations are substantially lower than the fractions of the passive compounds H_2O_2 and HO_2. The rate of formation of active atoms and radicals (carriers of the chain process) is increased because of the increase in gas temperature during the induction period (see Fig. 16) due to the exothermal reactions H + O_2 + M = HO_2 + M and $2HO_2 = H_2O_2 + O_2$ with the thermal effects $\Delta H = 204.4$ and 165.5 kJ/mole, respectively. The role of the chain branching reaction O_2 + H = OH + O (reaction No. 2) increases. The higher the concentration of H_2 in the syngas, the faster the increase in temperature and the more intense the increase in the concentration of H atoms and then of OH radicals and atomic oxygen. Vice versa, the concentrations of the H_2O_2 and HO_2 compounds decrease. Therefore, ignition in the syngas containing 20% of CO occurs faster approximately by a factor of 2.5 than in the case with 80% of CO.

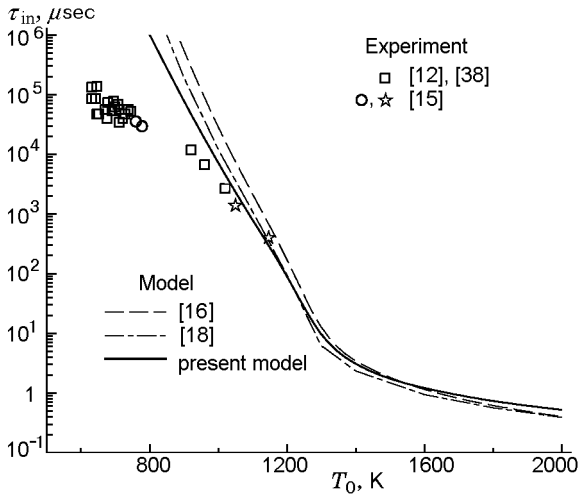

Fig. 17. Ignition delay times for the 4.1% H_2–5.3% CO–1.1% CO_2–18.8% O_2–70.7% N_2 mixture at $p_0 = 20$ atm versus temperature.

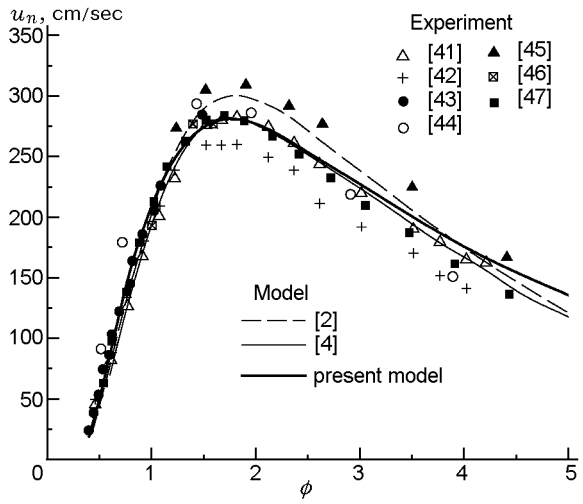

Fig. 18. Laminar flame velocity versus the fuel-to-air equivalence ratio in the H_2–air mixture at $p_0 = 1$ atm and $T_0 = 298$ K.

It should be noted that there are significant differences in the values of τ_{in} calculated by different reaction mechanisms and measured in the hydrogen–air mixture and in the mixture of the syngas and air both behind the reflected shock wave and in rapid compression machines at low temperatures ($T_0 \leqslant 900$ K) and high pressures ($p_0 \geqslant 5$ atm) [9, 13]. The same trend is also observed for the model considered in the present paper. The situation is illustrated in Fig. 17. It is seen that the difference between the values calculated by the models [16], [18] and by the present model, and those measured in [12, 15, 38] for the syngas–air mixture at $T_0 < 800$ K is more than tenfold. As was noted in [9], this can be related to proceeding of unsteady processes in shock tubes in the range of parameters considered or to specific features of gas-dynamic processes in the so-called rapid compression machines [11, 12], because these specific features are ignored in interpreting the experiment. There are also other possible reasons for the fact that the values of τ_{in} predicted by calculations are substantially higher than the experimental data. First of all, these are drawbacks of kinetic models, which ignore the possibility of formation of electronically excited $O_2(a^1\Delta_g)$ molecules and $O(^1D)$ atoms in reactions proceeding at low temperatures. For instance, these species can appear during interaction of H and HO_2: $H + HO_2 = H_2 + O_2(a^1\Delta_g)$ and $H + HO_2 = H_2O + O(^1D)$ [39, 40]. Taking into account that the rates of endoergic reactions with participation of $O_2(a^1\Delta_g)$ and $O(^1D)$ are considerably higher, especially at low temperatures, than the rates of the same reactions with non-excited particles, we can assume that formation of these species in the mixture can speed up chain reactions and reduce the values of τ_{in} predicted by advanced models.

The analysis of specific features of ignition of H_2–air and H_2–CO–air mixtures at low temperatures ($T_0 < 900$ K) and high pressures ($p_0 > 5$ atm) in shock tubes behind the front of the reflected shock wave and in rapid compression machines is outside the scope of the paper. In the general case, such an analysis should be performed within the framework of a more complicated gas-dynamic model that takes into account non-one-dimensionality and unsteadiness of the flow in such devices and the possibility of heterogeneous reactions on the reactor walls where the measurements are performed [9]. Recently published results of modeling ignition of the H_2–O_2 mixture at elevated pressures and low temperatures of the gas [10] indicate that the significant difference between the calculated values of τ_{in} and the experimental results in this range of p_0 and T_0 is not related to the gas-phase mechanism of chain reactions in H_2–air and H_2–CO–air mixtures.

2.3. Laminar Flame Propagation Velocity

In addition to the ignition delay time, another parameter often used for testing kinetic models is the measured laminar flame velocity u_n. Such measurements have been lately performed for H_2–O_2–N_2 (He) [14, 41–47] and H_2–CO–O_2–N_2 (He) [16, 48–50] mixtures in wide ranges of the fuel-to-air equivalence ratio and syngas composition (ratio of H_2 and CO fractions) both at atmospheric and elevated pressures.

Figure 18 shows the velocity u_n calculated by the kinetic models [2] and [4] and by the present model for

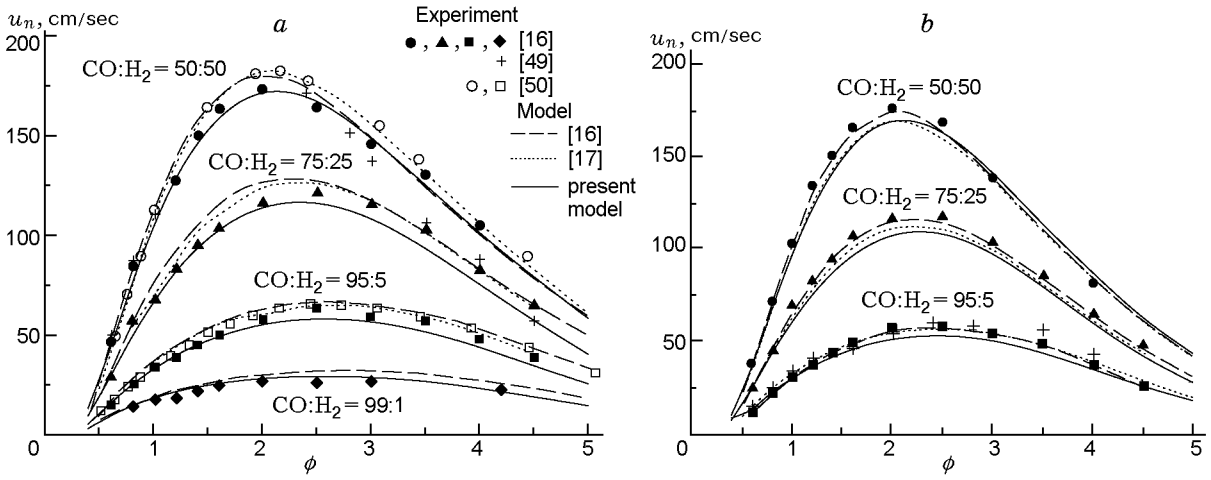

Fig. 19. Laminar flame velocity versus the fuel-to-air equivalence ratio in the syngas–air mixture at $T_0 = 298$ K and $p_0 = 1$ (a) and 2 atm (b).

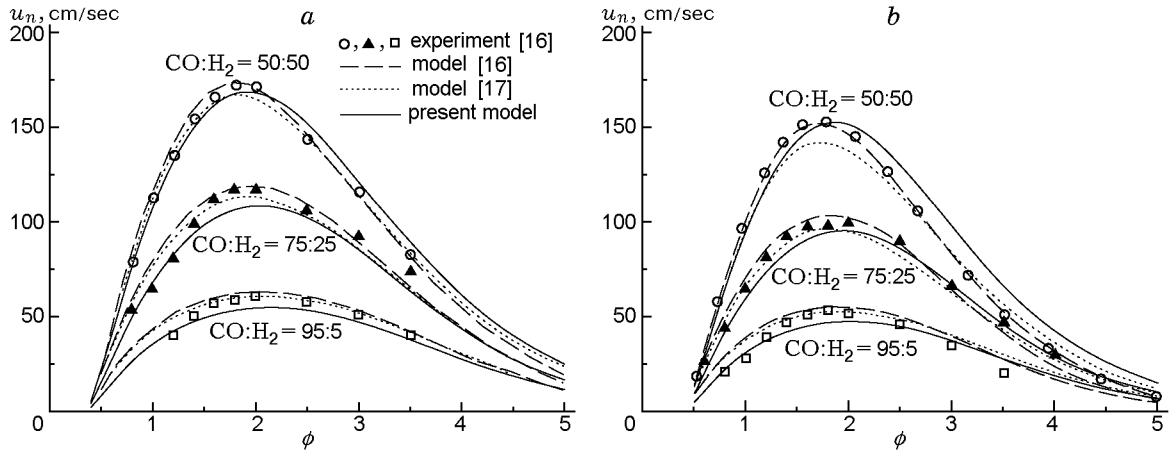

Fig. 20. Laminar flame velocity versus the fuel-to-air equivalence ratio in the CO–H_2–O_2–He mixture with different fractions of CO and H_2 in the syngas at $p_0 = 5$ (a) and 10 atm (b) and $T_0 = 298$ K.

the H_2–air mixture at $p_0 = 1$ atm and $T_0 = 298$ K, and also the experimental data [41–47]. It is seen that the predictions of all models considered are in good agreement with each other and with most measurements of u_n. Only the experimental data [42] obtained at the fuel-to-air equivalence ratio $\phi \geqslant 1.5$ are slightly lower than the results of other measurements. Note that all calculations of the flame velocity in our work were performed by the CHEMKIN IV software package [51], as well as in other works [3–5, 16–18] where the reaction mechanisms were tested on the basis of the measured values of u_n. The velocities u_n measured in [16, 49, 50] and calculated by the models [16] and [17] and by the present model in the syngas–air mixture at $p_0 = 1$ and 2 atm and $T_0 = 298$ K, different values of ϕ, and different ratios of CO and H_2 in the syngas are compared in Fig. 19. It is seen that the available experimental data are adequately described by all kinetic models considered. The same situation is observed for higher pressures $p_0 = 5$ and 10 atm at which u_n was measured in the H_2–CO–O_2–He mixture with different fractions of CO and H_2 [16] (Fig. 20).

Analyzing the dependences $u_n(\phi)$ in Figs. 18–20, we can conclude that the most adequate description of experimental data in H_2–CO–O_2–N_2 (He) mixtures at $T_0 = 298$ K in wide ranges of variation of ϕ and p_0, and the ratio of the CO and H_2 fractions in the syngas is provided by the kinetic model [17] and by the model discussed in the present paper. Therefore, it seems of interest to compare the accuracy of predictions of these

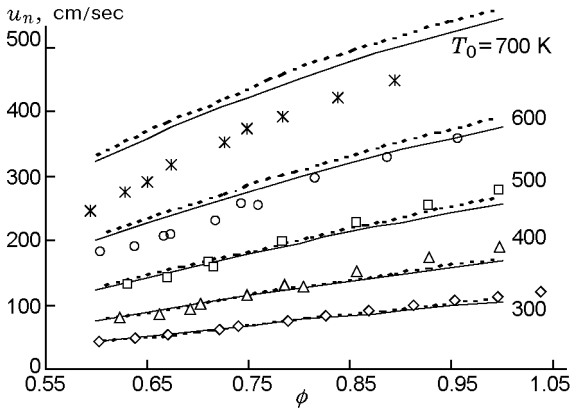

Fig. 21. Laminar flame velocity versus the fuel-to-air equivalence ratio for the CO–H_2–O_2–N_2 mixture (CO : H_2 = 50 : 50) at different temperatures and p_0 = 1 atm: the points are the experimental data [48]; the solid and dotted curves are the results calculated by the present model and by the model [17], respectively.

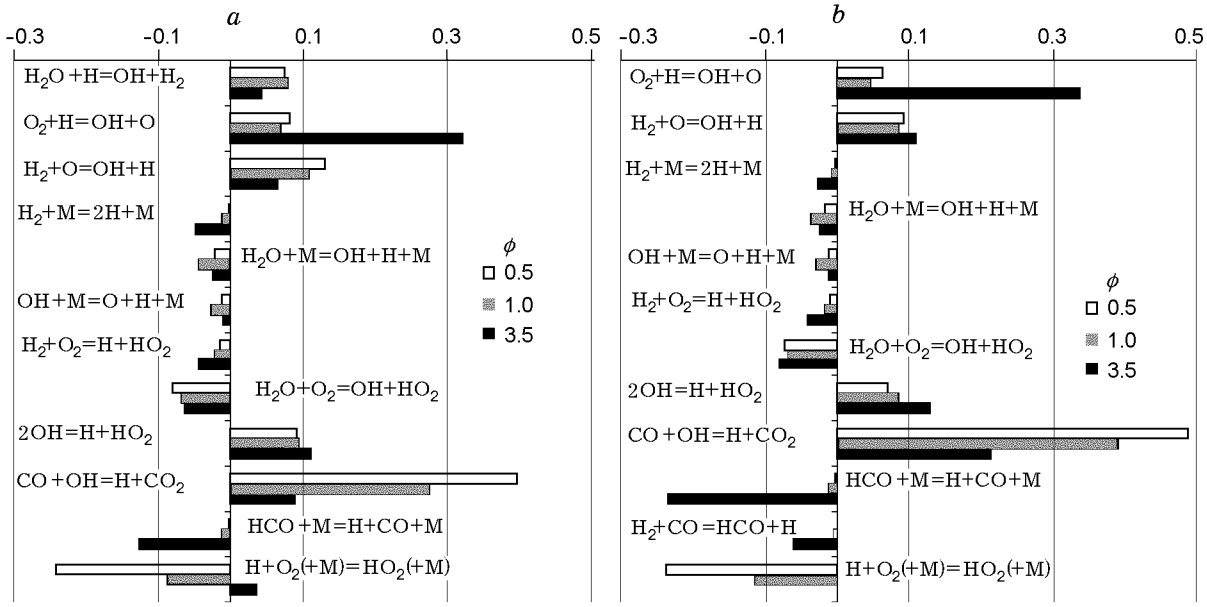

Fig. 22. Sensitivity of the velocity u_n to the contribution of individual reactions in the syngas–air mixture at p_0 = 1 atm, T_0 = 298 K, ratios CO : H_2 = 50 : 50 (a) and 75 : 25 (b), and different values of ϕ.

models both at T_0 = 298 K and at higher initial temperatures. The values of u_n in the H_2–CO–O_2–N_2 mixture at $T_0 > 298$ K were recently measured by Natarajan et al. [48]. The results measured in that work and calculated by the model [17] and by the present model for the syngas–air mixture at p_0 = 1 atm, ϕ = 0.6–1.0, and T_0 = 300, 400, 500, 600, and 700 K are shown in Fig. 21. It is seen that both models describe the experiment very well up to T_0 = 600 K. A certain difference between the measured and calculated values of u_n is observed only at T_0 = 700 K.

It is of interest to determine which reactions exert the most significant effect on the flame propagation velocity in the syngas–air mixture. This can be done through analyzing the sensitivity with the use of the present model, which is highly prognostic. The results of such an analysis for lean (ϕ = 0.5), stoichiometric (ϕ = 1.0), and rich (ϕ = 3.5) mixtures with different ratios of the CO and H_2 fractions in the syngas are shown in Fig. 22. It is seen that different reactions exert a dominating effect on the flame velocity, depending on the fuel-to-air equivalence ratio. Thus, the dominat-

ing reaction for the lean and stoichiometric mixtures is the chain propagation reaction $CO + OH = H + CO_2$, followed by the chain termination reaction $H + O_2 + M = HO_2 + M$. The reactions of chain branching $H_2 + O = OH + H$ and $O_2 + H = OH + O$ and the reactions with HO_2 formation, $2OH = H + HO_2$ and $H_2O + O_2 = OH + HO_2$, are also important. The situation is drastically different in the mixture enriched by the fuel ($\phi = 3.5$). The chain branching reaction $O_2 + H = OH + O$ is dominating here. The second important reaction is the recombination reaction $H + CO + M = HCO + M$ (chain termination reaction). It is only after this reaction that the reaction $CO + OH = H + CO_2$ occurs. As compared with the lean and stoichiometric mixtures, the influence of the reactions $H_2 + O = OH + H$, $2OH + H = HO_2$, and $H_2O_2 + O_2 = OH + HO_2$ is somewhat enhanced.

It is also seen that the degree of the influence of different reactions on the flame propagation velocity in the syngas–air mixture depends not only on the value of ϕ, but also on the ratio of the CO and H_2 fractions in the syngas. For instance, if the CO fraction in the syngas is reduced to 50%, then the role of reactions with participation of CO molecules (reaction Nos. 30 and 31) becomes less important, while the role of reactions responsible for the development of the chain process in the H_2–O_2 (air) mixture (reaction Nos. 2 and 3) increases. In this case, the reaction $H_2O + H = OH + H_2$ (reaction No. 1) makes a fairly significant contribution to u_n.

CONCLUSIONS

A kinetic model was developed to describe the processes of ignition and combustion of CO–H_2–O_2–N_2 (He or Ar) mixtures. The model ensures an adequate description of experimental data on the ignition delay time and laminar flame propagation velocity and also of the evolution of the most important species, which are carriers of the chain mechanism, during H_2 and syngas oxidation within wide ranges of temperature, pressure, and composition of the mixture. The mechanism proposed is applicable at $0.01 < p_0 < 60$ atm, $850 < T_0 < 2900$ K, and $0.3 < \phi < 5.0$. The kinetic model developed in the present work provides much better agreement with the measured ignition delay times than available reaction mechanisms.

The analysis shows that the degree of the influence of different reactions on the laminar flame velocity depends on the fuel-to-air equivalence ratio. Thus, the greatest effect on the flame velocity is exerted by the reaction $CO + OH = H + CO_2$ in the lean and stoichiometric mixtures and by the reaction $O_2 + H = OH + O$ in the rich mixture. The degree of the influence of different reactions also depends on the ratio between the CO and H_2 fractions in the syngas. The following reactions make the greatest contributions to the chain process development during ignition of the syngas–air mixture: chain initiation reaction $CO + O_2 = CO_2 + O$, chain branching reaction $O + H_2 = OH + H$, and chain termination reaction $H + O_2 + M = HO_2 + M$. The chain propagation reactions $H_2 + OH = H + H_2O$, $CO + OH = H + CO_2$, and $HCO + O_2 = HO_2 + CO$ also play a significant role. At moderate temperatures ($T_0 < 1100$ K), reactions of H_2O_2 formation and decomposition are also important. As for the flame propagation velocity, the role of different reactions depends on the ratio between the CO and H_2 fractions in the syngas proper. Despite the high prognostic capabilities of advanced kinetic models, there are some experiments performed at comparatively low temperatures ($T_0 \leqslant 970$ K) and high pressures ($p_0 > 5$ atm) in shock tubes, flow reactor, and rapid compression machines, that cannot be described by the kinetic models. Therefore, further theoretical and experimental studies of kinetic and gas-dynamic specific features of the ignition process in this range of gas parameters are needed.

This work was supported by the Russian Foundation for Basic Research (Grant Nos. 08-01-00808 and 08-08-00839) and by the Federal Targeted Program entitled "Academic and Teaching Staff of Innovative Russia" (State Contract No. 02.740.11.0074).

REFERENCES

1. D. J. Wilhelm, D. R. Simbeck, A. D. Karp, and R. L. Dickenson, "Syngas production for gas-to-liquids applications: technologies, issues and outlook," *Fuel Process. Technol.*, **71**, 139–148 (2001).
2. M. A. Mueller, T. J. Kim, R. A. Yetter, and F. L. Dryer, "Flow reactor studies and kinetic modeling of the H_2/O_2 reaction," *Int. J. Chem. Kinet.*, **31**, No. 10, 113–125 (1999).
3. J. Li, Z. Zhao, A. Kazakov, and F. L. Dryer, "An updated comprehensive kinetic model of hydrogen combustion," *Int. J. Chem. Kinet.*, **36**, 566–575 (2004).
4. M. O'Conaire, H. J. Curran, J. M. Simmie, et al., "A comprehensive modeling study of hydrogen oxidation," *ibid.*, pp. 603–622.
5. A. A. Konnov, "Remaining uncertainties in the kinetic mechanism of hydrogen combustion," *Combust. Flame*, **152**, 507–528 (2008).
6. A. M. Starik, N. S. Titova, L. V. Bezgin, and V. I. Kopchenov, "The promotion of ignition in a supersonic H_2–air mixing layer by laser-induced excitation of

O_2 molecules: Numerical study," *Combust. Flame*, **156**, No. 8, 1641–1652 (2009).
7. R. A. Yetter, F. L. Dryer, and H. Rabitz, "A comprehensive reaction mechanism for carbon monoxide/hydrogen/oxygen kinetics," *Combust. Sci. Technol.*, **79**, 97–128 (1991).
8. P. Saxena and F. A. Williams, "Testing a small detailed chemical-kinetic mechanism for the combustion of hydrogen and carbon monoxide," *Combust. Flame*, **145**, 316–323 (2006).
9. M. Chaos and F. L. Dryer, "Syngas combustion kinetics and applications," *Combust. Sci. Technol.*, **180**, 1053–1096 (2008).
10. G. A. Pang, D. F. Davidson, and R. K. Hanson, "Experimental study and modeling of shock tube ignition delay times for hydrogen–oxygen–argon mixtures at low temperatures," *Proc. Combust. Inst.*, **32**, 181–188 (2009).
11. G. Mittal, C. J. Sung, M. Fairweather, et al., "Significance of the HO_2 + CO reaction during the combustion of CO + H_2 mixtures at high pressures," *Proc. Combust. Inst.*, **31**, 419–427 (2007).
12. S. M. Walton, X. He, B. T. Zigler, and M. S. Wooldridge, "An experimental investigation of the ignition properties of hydrogen and carbon monoxide mixtures for syngas turbine applications," *Proc. Combust. Inst.*, **31**, 3147–3154 (2007).
13. F. L. Dryer and M. Chaos, "Ignition of syngas/air and hydrogen/air mixtures at low temperatures and high pressures: Experimental data interpretation and kinetic modeling implications," *Combust. Flame*, **152**, 293–299 (2007).
14. D. Bradley, M. Lawes, K. Liu, et al., "Laminar burning velocities of lean hydrogen–air mixtures at pressures up to 1.0 MPa," *Combust. Flame*, **149**, 162–172 (2007).
15. E. L. Petersen, D. M. Kalitan, A. B. Barrett, et al., "New syngas/air ignition data at lower temperature and elevated pressure and comparison to current kinetics models," *ibid.*, pp. 244–247.
16. H. Sun, S. I. Yang, G. Jomaas, and C. K. Law, "High-pressure laminar flame speeds and kinetic modeling of carbon monoxide/hydrogen combustion," *Proc. Combust. Inst.*, **31**, 439–446 (2007).
17. S. G. Davis, A. V. Joshi, H. Wang, and F. Egolfopoulos, "An optimized kinetic model of H_2/CO combustion," *Proc. Combust. Inst.*, **30**, 1283–1292 (2005).
18. J. Li, Z. Zhao, A. Kazakov, et al., "A comprehensive kinetic mechanism for CO, CH_2O, and CH_3OH combustion," *Int. J. Chem. Kinet.*, **39**, 109–136 (2007).
19. A. M. Starik, B. I. Lukhovitskii, and N. S. Titova, "Mechanisms of the initiation of combustion in $CH_4(C_2H_2)$/air/O_3 mixtures by laser excitation of the O_3 molecules," *Kinet. Katal.*, **48**, No. 3, 348–366 (2007).
20. J. V. Michael, J. W. Sutherland, L. B. Harding, and A. F. Wagner, "Initiation in H_2/O_2: Rate constants for $H_2 + O_2 \rightarrow H + HO_2$ at high temperature," *Proc. Combust. Inst.*, **28**, 1471–1478 (2000).
21. A. N. Pirraglia, J. V. Michael, J. W. Sutherland, and R. B. Klemm, "Rate coefficient of the $O + H_2 = OH + H$ reaction determined via shock tube-laser absorption spectroscopy," *J. Phys. Chem.*, **93**, 282 (1989).
22. D. L. Baulch, C. T. Bowman, C. J. Cobos, et al., "Evaluated kinetic data for combustion modeling," *J. Phys. Chem. Ref. Data*, **34**, No. 3, 757–1397 (2005).
23. X. You, H. Wang, E. Goos, et al., "Reaction kinetics of CO + $HO_2 \rightarrow$ products: ab initio transition state theory study with master equation modeling," *J. Phys. Chem. A*, **111**, 4031–4042 (2007).
24. L. V. Gurvich, I. V. Veyts, and C. B. Alcock, *Thermodynamic Properties of Individual Substances*, Hemisphere Publ. Co., New York (1989).
25. A. Burcat and B. Ruscic, "Third millennium ideal gas and condensed phase thermochemical database for combustion with updates from active thermochemical tables," ANL-05/20 and TAE 960 Technion-IIT, Aerospace Engineering, and Argonne National Laboratory, Chemistry Division (2005).
26. J. T. Herbon, R. K. Hanson, D. M. Golden, and C. T. Bowman, "A shock tube study of the enthalpy of formation of OH," *Proc. Combust. Inst.*, **29**, 1201–1208 (2002).
27. R. A. Yetter, F. L. Dryer, and H. Rabitz, "Flow reactor studies of carbon monoxide/hydrogen/oxygen kinetics," *Combust. Sci. Technol.*, **79**, 129–140 (1991).
28. R. K. Lyon, J. E. Hardy, and W. V. Holt, "Oxidation kinetics of wet CO in trace concentrations," *Combust. Flame*, **61**, 79–86 (1985).
29. R. R. Craig, "A shock tube study of the ignition delay of hydrogen-air mixtures near the second explosion limit," Report No. AFAPL-TR-66-74 (1966).
30. A. D. Snyder, J. Robertson, D. L. Zanders, and G. B. Skinner, "Shock tube studies of fuel-air ignition characteristics," Report No. AFAPL-TR-65-93 (1965).
31. M. Slack and A. Grillo, "Investigation of hydrogen-air ignition sensitized by nitric oxide and nitrogen dioxide," NASA Report No. CR-2896 (1977).
32. E. Schultz and J. Shepherd, "Validation of Detailed Reaction mechanisms for detonation simulation," Tech. Report No. FM 99-5: 230, Cal. Inst. of Tech. Graduate Aeronautical Lab. (2000).
33. K. A. Bhaskaran, M. C. Gupta, and Th. Just, "Shock tube study of the effect of unsymmetric dimethyl hydrazine on the ignition characteristics of hydrogen–air mixtures," *Combust. Flame*, **21**, 45–48 (1973).
34. M. W. Slack, "Rate coefficient for $H + O_2 + M = HO_2 +$ M evaluated from shock tube measurements of induction times," *Combust. Flame*, **28**, 241–249 (1977).
35. A. M. Dean, D. C. Steiner, and E. E. Wang, "A shock tube study of the H_2/O_2/CO/Ar and H_2/N_2O/CO/Ar systems," *Combust. Flame*, **32**, 73–83 (1978).

36. W. C. Gardiner, M. McFarland, K. Morinaga, et al., "Ignition delays in H_2–O_2–CO–Ar mixtures," *J. Phys. Chem.*, **75**, 1504–1509 (1971).
37. E. L. Petersen, D. F. Davidson, M. Röhrig, and R. K. Hanson, "High-pressure shock-tube measurements of ignition times in stoichiometric H_2–O_2–Ar mixtures," in: *Proc. of the 20th Int. Symp. on Shock Waves*, Pasadena (1995), pp. 941–946.
38. W. T. Peschke and L. J. Spadaccini, "Determination of autoignition and flame speed characteristics of coal gases having medium heating values," Electric Power Research Inst., Report EPRI AP-4291 (1985).
39. M. Filatov, W. Reckien, S. D. Peyerimhoff, and S. Shaik, "What are the reasons for the kinetic stability of a mixture of H_2 and O_2?" *J. Phys. Chem.*, **104**, 12014–12020 (2000).
40. S. H. Mousavipour and V. Saheb, "Theoretical study on the kinetic mechanism of H + HO_2 reaction," *Bull. Chem. Soc. Jpn.*, **80**, No. 10, 1901–1913 (2007).
41. S. D. Tse, D. L. Zhu, and C. K. Law, "Morphology and burning rates of expanding spherical flames in H_2/O_2/inert mixtures up to 60 atmospheres," *Proc. Combust. Inst.*, **28**, 1793–1800 (2000).
42. K. T. Aung, M. I. Hassan, and G. M. Faeth, "Flame stretch interactions of laminar premixed hydrogen/air flames at normal temperature and pressure," *Combust. Flame*, **109**, 1–24 (1997).
43. C. K. Law, "A compilation of experimental data on laminar burning velocities," in: N. Peters and B. Rogg (eds.), *Reduced Kinetic Mechanisms for Applications in Combustion Systems,* Springer-Verlag, Berlin (1993), pp. 15–26.
44. T. Iijima and T. Takeno, "Effects of temperature and pressure on burning velocity," *Combust. Flame*, **65**, 35–43 (1986).
45. F. Takahashi, M. Mizomoto, and S. Ikai, "Numerical studies on the structure of two-dimensional H_2/air premixed jet flame," *Alternative Energy Sources III*, **5**, 447–457 (1983).
46. C. K. Wu and C. K. Law, "On the determination of laminar flame speeds from stretched flames," in: *Proc. Combust. Inst.*, **20**, 1941–1949 (1984).
47. D. R. Dowdy, D. B. Smith, S. C. Taylor, and A. Williams, "The use of expanding spherical flames to determine burning velocities and stretch effects in hydrogen/air mixtures," in: *Proc. Combust. Inst.*, **23**, 325–332 (1991).
48. J. Natarajan, T. Lieuwen, and J. Seitzman, "Laminar flame speeds of H_2/CO mixtures: effect of CO_2 dilution, preheat temperature, and pressure," *Combust. Flame*, **151**, 104–119 (2007).
49. M. I. Hassan, K. T. Aung, and G. M. Faeth, "Properties of laminar premixed CO/H_2/Air flames at various pressures," *J. Propulsion Power*, **13**, No. 2, 239–245 (1997).
50. I. C. McLean, D. B. Smith, and S. C. Taylor, "The use of carbon monoxide/hydrogen burning velocities to examine the rate of the CO + OH reaction," in: *Proc. Combust. Inst.*, **25**, 749–757 (1994).
51. R. J. Kee, F. M. Rupley, J. A. Miller, et al., CHEMKIN Collection, Release 3.6, Reaction Design, Inc., San Diego, CA (2000).